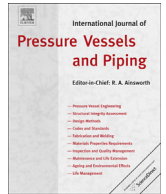




Contents lists available at ScienceDirect

International Journal of Pressure Vessels and Piping

journal homepage: www.elsevier.com/locate/ijpvp

Material and residual stress considerations associated with the autofrettage of weld clad components

G. Benghalia*, J. Wood

University of Strathclyde, 75 Montrose Street, Glasgow G1 1XJ, UK

ARTICLE INFO

Article history:
Available online xxx

Keywords:
Weld cladding
Residual stress
Autofrettage
Finite element analysis

ABSTRACT

A fatigue-resistant cladding concept confirms the presence of compressive residual stresses in a cylinder weld clad with 17–4 PH stainless steel while tensile residual stresses exist in an Inconel 625 clad layer. In this study, autofrettage of an Inconel 625 thick-walled clad cylinder is investigated with modified residual stress distributions obtained indicating that tensile residual stresses throughout the clad layer are transformed to compressive in nature, discontinuity stresses at the clad/substrate interface are almost entirely eliminated and compressive residual stresses exist to a depth of around 18 mm. An alternative clad material, 17–4 PH stainless steel, is investigated resulting in compressive residual stresses in the clad layer without the need for autofrettage. The complexity of modelling a martensitic stainless steel is discussed and sensitivity studies undertaken to illustrate the influence of coefficient of thermal expansion on resulting residual stresses. Strain hardening effects and the assumption of an idealised interface are discussed. Contour method measurements prove that discontinuity stresses are reduced in reality due to alloying and diffusion effects, highlighting also the need for further characterisation of 17–4 PH. Additional considerations such as the weld clad profile and process parameters are briefly discussed.

© 2016 The Authors. Published by Elsevier Ltd. This is an open access article under the CC BY license (<http://creativecommons.org/licenses/by/4.0/>).

1. Introduction

The issue of fatigue failure in weld clad components, such as pipelines utilised in the oil and gas industry, has prompted an investigation into a fatigue-resistant cladding technology to enhance the performance of these components. Fatigue of welded joints and dissimilar material joints have been studied with focus herein placed on weld cladding of 4330 low alloy carbon steel. Two clad materials are investigated, namely nickel-chromium-based superalloy Inconel 625 and 17–4 PH stainless steel.

The application of a coating or cladding to a substrate using a thermal deposition process results in a self-equilibrating residual stress distribution primarily due to the thermal cycle and the associated metallurgical changes during the melting, deposition, solidification and cooling of the material. The arising constraint on differential expansion and associated phase changes results in residual stresses, with material property variation with time and temperature additionally influencing the residual stress state.

Dissimilarity in properties between substrate and clad materials further affects the self-equilibrating residual stress field. The nature of the residual stresses in the coating/cladding may be tensile or compressive depending on the characteristics of the dissimilar materials and the process involved. Due to the interest in fatigue performance, the arising residual stress state post-cladding is evaluated.

Tensile residual stresses are commonly induced through many welding and machining processes, therefore providing an undesirable stress state at the surface of the component. It is also common that maximum operational stresses occur at the surfaces of components. Cladding and coating processes often lead to large discontinuity stresses at the interface and fatigue cracking can also occur at this location. Therefore, the aim of this concept is to obtain a compressive residual stress at the component surface and to as great a depth as possible into the clad surface and substrate while reducing or eliminating discontinuity stresses. Finite element models of the weld cladding process, along with experimental validation using the incremental hole-drilling method (ICHD), demonstrate the ability to apply a fatigue-resistant cladding process on 4330 steel using 17–4 PH with compressive residual stresses resulting. However, tensile residual stresses are obtained in

* Corresponding author.

E-mail address: gladys.benghalia@strath.ac.uk (G. Benghalia).

the case of an Inconel 625 clad [1]. Therefore a post-cladding autofrettage process is under investigation in an attempt to modify these stresses into beneficial compressive residual stresses. Although weld cladding and autofrettage are commonly utilised processes, it appears that there have been no previous studies on the effects of autofrettage of weld cladding [2].

The concept is not limited to the weld cladding of 4330 steel with Inconel 625 or 17–4 PH, with potential applicability to other coatings and claddings applied to substrates for the purposes of improving erosion, corrosion, thermal, optical and other performance measures, particularly where cyclic loading is present. Similar characteristics have been observed in laser cladding using these material combinations, not reported herein.

1.1. Weld clad simulation review

A simplified finite element simulation of a weld clad cylinder was obtained through a two-dimensional axisymmetric model assuming the entire clad layer is deposited on the inner diameter of a cylinder in one step. A thermal transient stress analysis consisted of a pipe pre-heated to one of two temperatures, 150 or 300 °C, prior to the application of the weld material at melt temperature. The entire component was then subjected to slow cooling on the inner and outer surfaces using a convective heat transfer coefficient $h = 10 \text{ W/m}^2 \text{ K}$. Latent heat effects were neglected and radial edges of the model were insulated to simulate no axial heat transfer. A bulk temperature of 25 °C was applied, radiation heat transfer was neglected and Poisson's ratio assumed constant with time and temperature. Plane strain conditions were applied on radial lines and an elastic-perfectly plastic material model assumed with the use of temperature dependent thermal and mechanical material properties. These properties were experimentally obtained for clad and heat-affected zone (HAZ) regions to ensure accurate capturing of the material behaviour, most crucially ensuring phase changes are accounted for where relevant.

The assumptions made in terms of model geometry and behaviour are consistent with the experimental weld cladding process, reflected in the results discussed.

Fig. 1 shows the clad cylinder dimensions in millimetres and the associated axisymmetric finite element model. Fig. 2 shows the results for the as-clad self-equilibrating residual stress distribution along the axisymmetric model for an Inconel 625 clad on 4330 steel.

The clad model initially produces high biaxial tensile residual stresses in the clad layer and into the substrate. Hoop stresses in the clad layer are tensile for both substrate pre-heat temperature values and the effect due to pre-heat temperature is seen to be negligible. Due to the dissimilarity in the materials, a discontinuity stress will also invariably exist at the interface between the cladding/coating and the substrate. The discontinuity stress can be significantly higher than the stress in the clad material, as is also shown to be the case here. From a fatigue viewpoint, cracks may

develop at either the clad/coating surface or the interface as mentioned previously, depending on the nature of the combined residual and operational stress distributions and the fatigue strength of the as-deposited materials involved.

2. Validating 'as-clad' residual stresses

Limited validation of simulation residual stresses to a depth of 1 mm was obtained using the incremental centre hole drilling (ICHD) method. ICHD is a relaxation method which measures strains in the vicinity of a drilled hole through the application of a strain gauge rosette on the surface of the component [3]. These strain values are then converted into stresses, with the comparison between simulation and experimental hoop stress values shown in Fig. 3. Results are shown for a 4330 steel cylinder with pre-heat temperature 300 °C externally clad with Inconel 625, with the same dimensions and clad thickness as an internally clad cylinder.

Machining of the weld profile was required to enable the strain gauge rosette to be laid on the surface of the weld clad cylinder and these surface effects can be seen in hoop stress values in the first 200 microns from the clad surface. Overall, however, correlation between hoop stress values obtained through simulation and experimental means is good. Experimental measurements also established the axisymmetric nature of the results.

Further model validation included autofrettage predictions for a pressurized plain cylinder, for which good agreement with theory was obtained as presented herein.

3. Modifying 'as-clad' residual stress distribution

In terms of the NACE International regulations [4], the use of Inconel 625 as a weld clad material presents no issues in compliance with the regulations. The beneficial properties of erosion and corrosion resistance provided by Inconel 625 are recognized and therefore post-cladding processes are investigated with a view to improving the residual stress state and ultimately the fatigue-resistance in the case of 4330 steel clad with Inconel 625.

There are three characteristics of the typical as-clad residual stress distribution shown in Fig. 4 that could be modified in a manner that would improve the fatigue performance of the component:

- A: Transformation of the tensile residual stress to a compressive residual stress, with as high a magnitude as possible, throughout the thickness of the clad. This would reduce the likelihood of surface cracks initiating and propagating, with this protection offered in an erosive/corrosive environment until the clad thickness has been removed.
- B: Elimination, or at least a decrease in the level, of tensile discontinuity stress at the interface, leading to the reduction of the likelihood of cracks initiating and propagating at the interface between the clad and substrate.

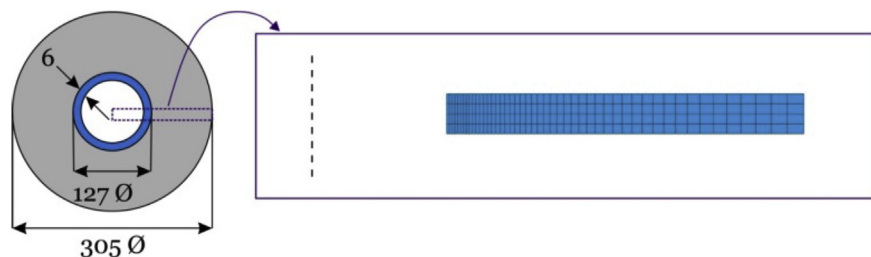


Fig. 1. Axisymmetric finite element model – clad deposition on inner diameter of cylinder (dimensions in mm).

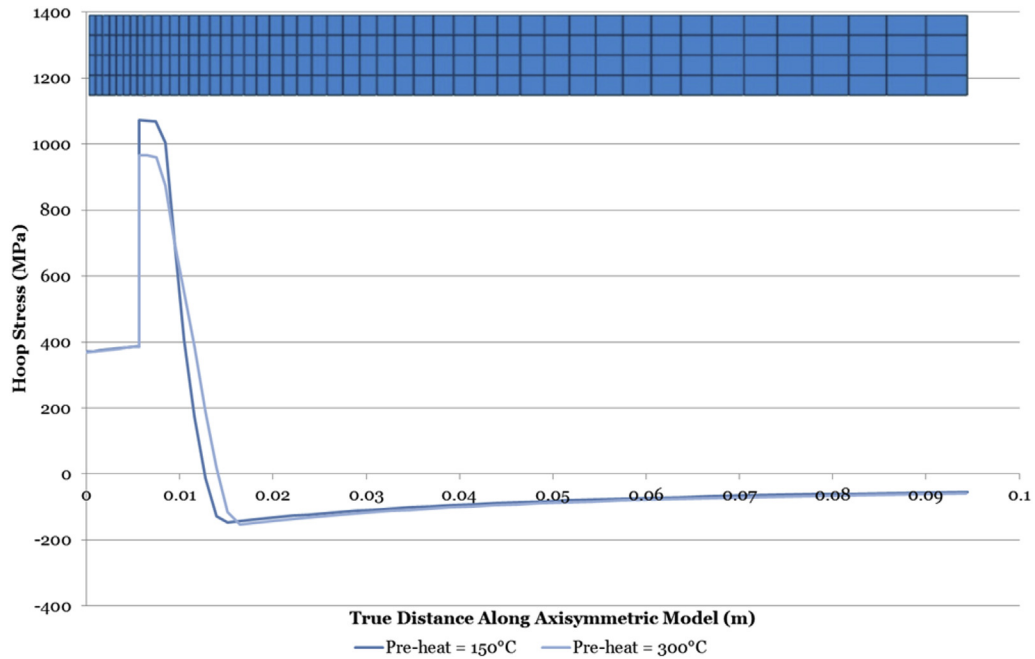


Fig. 2. Hoop residual stress distribution – Inconel 625 clad cylinder.

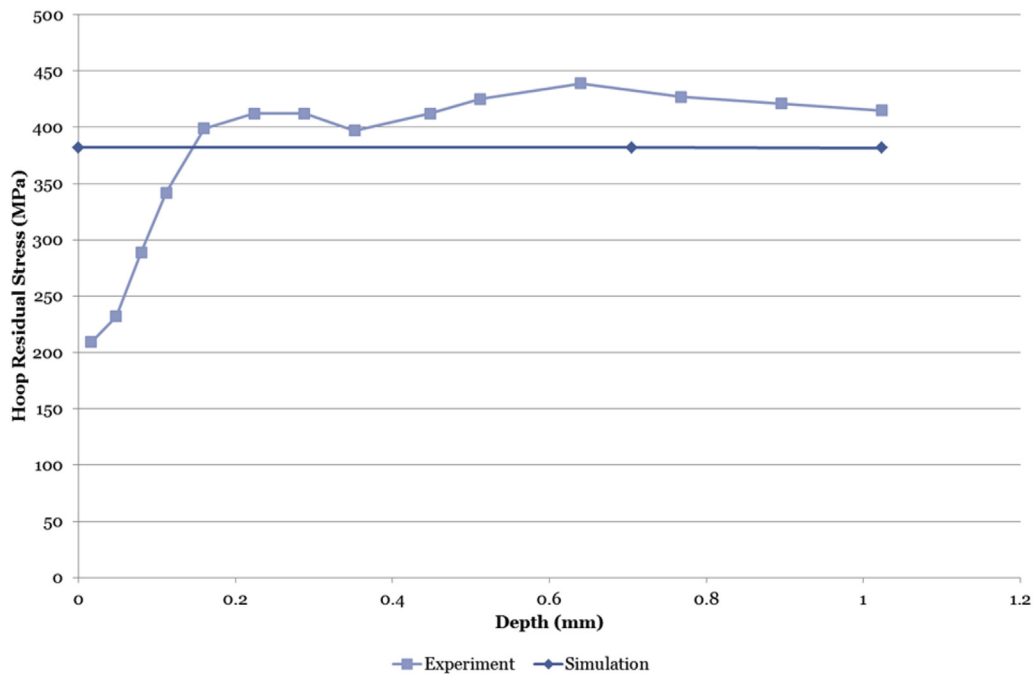


Fig. 3. Comparison of simulation and experimental hoop residual stress values – Inconel 625 clad cylinder.

C: Assuming that A is achieved, it would be desirable for the cross-over point between compressive and tensile residual stresses to be at as great a depth as possible. While not as significant as A and B this would be desirable due to the reduction in crack initiation and propagation potential to a greater depth below the surface and interface. This would also provide protection to a greater depth in an erosion-corrosion environment.

To achieve these three goals, there are various operations that could be implemented depending on the whether this modification

should take place in the design, process or post-cladding phase. Weld and laser cladding investigations have confirmed that goal A can be achieved through careful selection of substrate and clad materials, with significant compressive residual stresses obtained using a 17–4 PH clad on 4330 steel [5]. Altering process parameters allows further adjustment of the residual stress state in a clad component. Goal B would be possible by grading the transition at the interface between the dissimilar materials. The number and thickness of transition layers is a variable that will be both application and process dependent. It is unknown at this point in time as

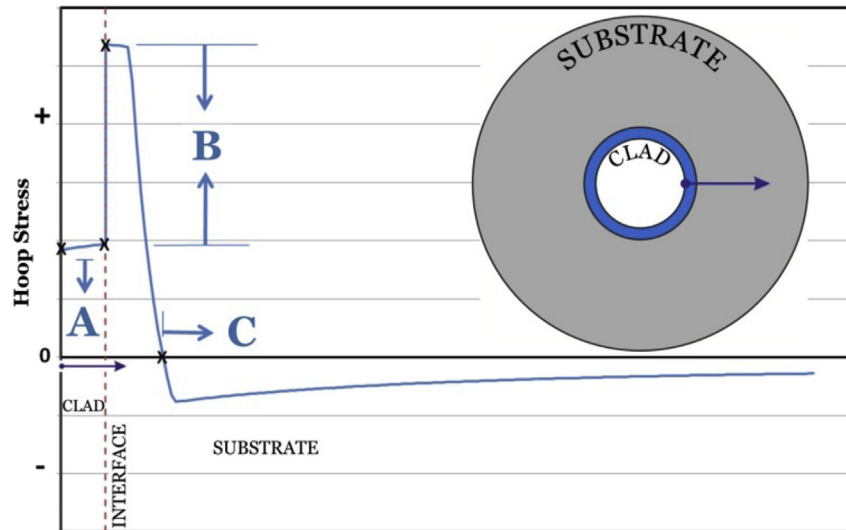


Fig. 4. Elements of the fatigue-resistant cladding concept.

to the effect such grading would have on goal A.

Investigation of the effects of heat-treatment on the simulation model have demonstrated the potential to adjust the magnitude and depth of residual stresses through control of the rate of heat transfer in radial and axial directions in a thick-walled cylinder. The effect of this operation post-cladding is unknown, however, the possibility of generating compressive residual stresses at the surface of the clad component suggests that this would be worthy of further investigation, examining the effects such an operation would have on both the residual stress state and the metallurgy of the joint.

There are various post-cladding operations that could be utilised to impact goals A, B and C to varying degrees. Shot peening, for example, is known to induce compressive residual stresses in a thin surface layer, which would therefore achieve goal A to some extent, however goals B and C would not be achieved through such relatively shallow surface treatments. Due to the effects of shot peening only leading to increased fatigue performance in a thin surface layer, it is unlikely that these effects will be adequate in an aggressive erosive/corrosive environment. One method with potential to introduce significant change is mechanical autofrettage [6].

4. Autofrettage theory for a pressurized cylinder

The process of autofrettage induces a compressive residual stress through the application of a pressure in this case to increase the fatigue life of a component. Subjecting a compound cylinder to autofrettage results in that cylinder possessing a higher fatigue resistance compared with a homogeneous cylinder of the same dimensions [7]. A clad cylinder is in essence similar to a compound cylinder due to the component consisting of an internally clad cylinder with an external cylinder, namely the substrate, and an internal cylinder, namely the clad layer. During weld cladding a shrinkfit process effectively takes place between the substrate and the clad layer. The difference is of course that in the clad case there is a welded joint between the two cylinders as opposed to a shrink fit. Therefore autofrettage of the clad cylinder is regarded as a beneficial area of study.

To determine the correct autofrettage pressure for a certain component, it must be considered at what pressure the wall of the cylinder will be in a state of plastic flow. A cylinder subjected to

internal pressure will initially begin to experience yielding at a pressure $p_{Y.P.}$ given by:

$$p_{Y.P.} = \tau_{Y.P.} \left[\frac{b^2 - a^2}{b^2} \right] \quad (1)$$

$\tau_{Y.P.}$ is the shear stress at the yield point, a the inner radius and b the outer radius.

The maximum pressure that the component can withstand, known as the bursting pressure p_{burst} , is related in the following manner to the ultimate tensile strength $\sigma_{ult.}$ and the ratio of outer to inner radii K [8]:

$$p_{burst} = \sigma_{ult.} \log_e K \quad (2)$$

Due to the self-equilibrating nature of residual stresses, cladding residual stresses can be assumed to have no effect on the theoretical burst pressure, likewise is the case with stresses arising through a shrinkfit effect or autofrettage process. Throughout this investigation an elastic-perfectly plastic material has been assumed.

The pressure required for the entire wall of a plain cylinder to be brought into a state of plastic flow is equal to the negative of the radial stress σ_{ra} at the inner surface [8]:

$$p_u = -\sigma_{ra} = -2\tau_{Y.P.} \log_e \frac{a}{b} \quad (3)$$

The geometric mean radius $R_{G.M.}$ is given as the greatest depth to which yielding is safely permissible [9]:

$$R_{G.M.} = \sqrt{R_1 R_2} \quad (4)$$

The maximum autofrettage pressure can then be calculated based on the geometric mean radius using the following equation given by Hearn, where R_1 and R_2 are the internal and external radii respectively.

For a pressurized plain cylinder, yielding to any radius R_p can be obtained by applying the appropriate autofrettage pressure P_A , calculated through the equation provided by the High Pressure Technology Association code of practice [9]:

$$P_A = \frac{\sigma_y}{2} \left[\frac{K^2 - m^2}{K^2} \right] + \sigma_y \log_e m \quad (5)$$

where $K = R_2/R_1$ and $m = R_p/R_1$.

The theory presented does not account for the bimetallic nature of the weld clad cylinder. In the clad cylinder, the high-strength substrate will slow the progress of yield through the lower strength clad as there is a greater constraint on the radial expansion of the cylinder. Due to this bimetallic nature of the cylinder, manual adjustment of the input pressures was required to obtain pressures adequate to yield to the desired depth for a stress-free compound cylinder. In the case of a weld-clad model with an induced stress state this requires further adjustment.

For the case of a 17–4 PH clad with a much larger yield stress, the pressure required for autofrettage would be much larger to allow the resulting compressive residual stress field from the cladding operation of around -400 MPa to be taken up to the yield value of 17–4 PH (994 MPa). This is vastly different to beginning with a stress-free state.

The Inconel 625 clad has a tensile residual stress of around 400 MPa post-cladding and therefore would not require as high an autofrettage pressure, indicating that autofrettage of this case should be more easily attainable.

5. Simulating the autofrettage process

Initially, an autofrettage pressure was applied to a stress-free cylinder to verify the correct implementation of the autofrettage process. As a benchmark, an unclad low alloy carbon steel cylinder was analysed and compared to the theoretical solution presented in the previous section, providing satisfactory correlation.

The weld clad model is subjected to a pressure on the inside surface, using the as-clad residual stress state shown in Fig. 2.

Two pressures are applied, a low and a high pressure to investigate the effects of applied pressure and the scope of autofrettaging the clad cylinder. Both the discontinuity stresses and surface stresses are of interest in analysis of the results.

The cladding simulation is performed with the clad material deposited at melt temperature onto the pre-heated cylinder. The whole model is then cooled to room temperature prior to an autofrettage pressure being applied in a ramped manner at the desired value. Model geometry and properties are shown in Fig. 5.

Simulation using estimated pressure values indicated that a pressure of 400 MPa would be required to yield to a depth of approximately 5 mm.

Low and high autofrettage pressures of 400 MPa and 800 MPa respectively are applied, chosen to ensure suitable depths of yielding in the clad cylinder. The pressure is then removed by ramping the pressure back to zero and residual stresses investigated. The Von Mises yield criterion is used in the simulation.

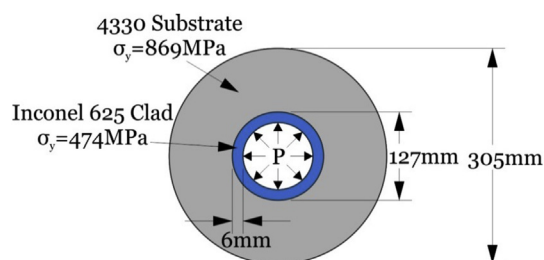


Fig. 5. Autofrettage of clad cylinder – illustrating model geometry and yield stress values.

6. Results

The results for a 4330 steel thick-walled cylinder clad with Inconel 625 are presented below.

Hoop stresses possess their maximum compressive value at the inner surface, reflected in the post-autofrettage curve for a low autofrettage pressure in Fig. 6.

Examining the hoop stress distribution, it is observed that the initial damaging tensile residual stress throughout the clad layer has been transformed to beneficial high compressive levels at both autofrettage pressures. Applying a low autofrettage pressure of 400 MPa produces high compressive residual stresses in the clad layer and lowers tensile residual stresses in the substrate, with discontinuity stresses at the clad-substrate boundary also reduced. Applying a high autofrettage pressure of 800 MPa produces high compressive residual stresses in the clad layer and into the substrate alongside a compressive discontinuity stress at the interface. This compressive discontinuity stress may be desirable depending on the metallurgy of the joint and the resulting mechanical properties achieved for the dissimilar materials at the joint. Although a compressive discontinuity stress is favourable in preventing crack initiation at this location, the issue of dissimilar materials and therefore dissimilarity in material properties remains.

Compressive residual hoop stresses exist to a depth of around 18 mm, or three clad layer thicknesses, for the case of high autofrettage pressure. The same level of compressive residual hoop stresses result in the clad layer for both autofrettage pressures as shown in Fig. 6 due to the use of the same yield in tension and compression.

Calculating the theoretical autofrettage pressure required to yield to a depth of 18 mm using the equation presented previously to yield to any radius results in a value of 734 MPa. This value is comparable with the high autofrettage pressure of 800 MPa illustrating that yielding into the substrate allows the use of theoretical calculations to provide pressure indications. The discrepancy in pressure values also confirms the expectation that the high-strength substrate slows the progression of yield through the lower strength clad material as stated previously.

As residual stresses are in their nature self-equilibrating, it was verified that residual stress path plots resulted in self-equilibration of residual stresses. If however, any machining or cutting of the cylinder were to take place, the self-equilibrating stress distribution would be altered and this must be considered in the manufacturing process and the preparation of the component for operation.

As mentioned previously, yielding to the geometric mean radius was also considered as this is generally the maximum allowable autofrettage radius presented in the standards [9]. However, it is recognized that from a practical and economic point of view, the high autofrettage pressure of 800 MPa utilised in this simulation is demanding.

7. Alternative clad material

It has been shown in Fig. 2 that cladding a 4330 substrate with nickel-based superalloy Inconel 625 yields tensile residual stresses in the clad layer. It is also known that a dominating factor in the generation of residual stresses due to coatings in general is the coefficient of thermal expansion (CTE) [10] due to this property being the coupling between thermal and mechanical behaviour [11]. This therefore indicates that careful selection of materials based on the relationship between clad and substrate coefficient of thermal expansion values could yield compressive residual stresses in the clad layer. A second clad material, namely 17–4 PH stainless steel, was investigated with the aim of achieving this. Undertaking

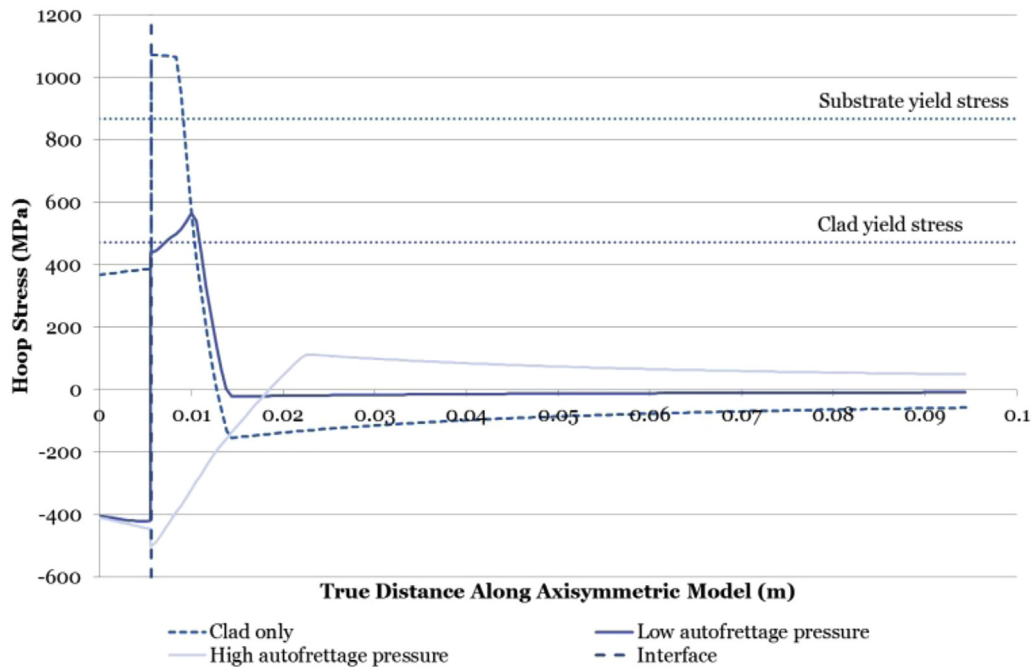


Fig. 6. Effects of autofrettage on hoop residual stress – Inconel 625 clad cylinder.

similar simulation studies utilizing thermal and mechanical temperature dependent properties obtained experimentally, the residual stress distributions along the central horizontal path in the axisymmetric model were obtained for the same pre-heat temperatures as previously: 150 °C and 300 °C. The hoop stress distribution for a 17–4 PH weld clad layer deposited on the outer diameter of a 4330 cylinder is shown in Fig. 7. It can be seen that this differs greatly in comparison with the previous residual stress distribution obtained when cladding with Inconel 625. Compressive residual stresses are present throughout the entire clad layer in

the region around the yield stress of the material, this value experimentally obtained as 994 MPa. A sharp discontinuity stress is again present resulting in tensile residual stresses at the interface in the substrate material. Tensile residual stresses are present in the entire substrate.

Fig. 7 proves the potential to obtain compressive residual stresses in the clad layer when utilizing a particular combination of clad and substrate materials. However experimental residual stress measurements obtained using ICHD indicate compressive residual stresses around –400 MPa in the clad layer as shown in Fig. 8. This

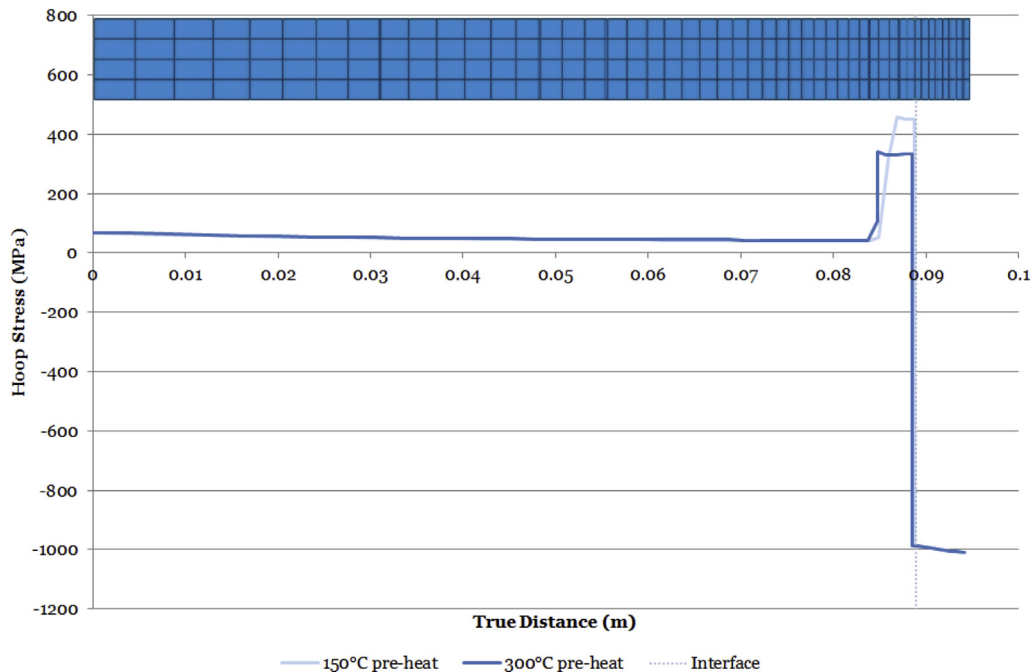


Fig. 7. Hoop residual stress distribution – 17–4 PH clad cylinder.

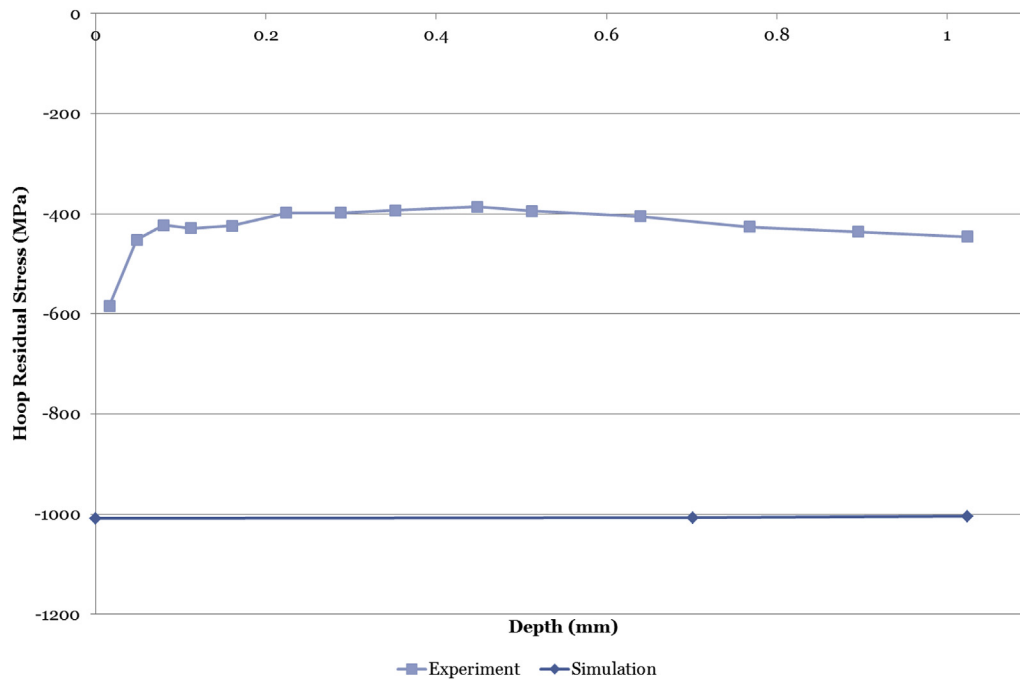


Fig. 8. Comparison of simulation and experimental hoop residual stress values – 17–4 PH clad cylinder.

suggests that the simulation model cannot accurately capture the residual stress distribution resulting due to the real weld cladding process and material effects such as alloying and diffusion which are not accounted for in the simulation.

7.1. Capturing the martensitic transformation

It is crucial in modelling residual stress generation that accurate temperature-dependent thermal and mechanical properties are input as these can heavily impact the resulting residual stress state. Good correlation has been obtained in the case of an Inconel 625 clad on 4330. Inconel 625 is an austenitic nickel-chromium-based superalloy while 17–4 PH is a precipitation hardening martensitic stainless steel. The complexity of modelling the martensitic transformation is well known and requires in-depth knowledge of the occurrence of the martensitic transformation specific to the case in question.

A significant experimental programme has been undertaken to obtain temperature-dependent thermal and mechanical properties for 4330, Inconel 625 and 17–4 PH. As previously mentioned, the CTE is a dominant factor in the generation of residual stresses and it is known that the limitation of the Netzsch DIL 402C [12] utilised in obtaining temperature-dependent CTE values does not capture the cooling rate experienced during the cladding process. During the welding process it is known that initial cooling rates will be very high, studies have been conducted into dilatation during cooling at a rate of 234 K/s [13].

The equipment utilised, catering more accurately for heating of the sample, was limited to a cooling rate of 5 K/min to provide the greatest range of data. It is therefore clear that the data obtained will not capture the CTE upon cooling for a welding process. The original data obtained is shown in Fig. 9. This figure shows the data used to investigate the effects of modifying the CTE upon cooling. The sharp decrease in CTE around 200 °C shows the location of the martensitic transformation and the corresponding effects on CTE values. It should be emphasized at this point that the CTE during heating and cooling for Inconel 625 remained very similar, with

little to no change to the linear trend of increasing CTE with temperature. This demonstrates the ability to correlate CTE variations with residual stress generation.

It would also be possible to account for the martensitic transformation through use of the Koistinen-Marburger function accounting for the fraction of martensite at a particular temperature upon cooling. In terms of integrating the martensitic transformation into a finite element simulation, the full volumetric change strain can be considered for the material in question and multiplied by the change in martensite fraction in a specific time step to result in the associated strain change at that time step [14].

It is the volume change associated with the martensitic transformation upon cooling of a martensitic steel that induces the compressive residual stress [15], [16]. The formation of martensite is encouraged by quenching processes, the nature of which arises through the rapid cooling during the weld cladding process. A martensitic microstructure is said to result if the material experiences cooling from the austenitic condition to below the martensite start temperature within less than 10 s [13].

The use of an interpass temperature during cladding is common practice. However this also impacts the resulting phases and residual stress states. If the interpass temperature is chosen such that it is above the martensite start temperature then the entire weld material will not undergo martensitic transformation until after the welding process has been completed. This would then encourage compressive residual stresses in the fusion zone. An interpass temperature below that of the martensite start temperature would lead to tempering of previously deposited passes, decreasing the compressive region [17].

It has been mentioned by Todinov that the development of compressive residual stresses is hindered through delaying the martensitic transformation at the surface [18]. It is further mentioned that a large temperature interval, that is a high transformation start temperature and a low transformation end temperature, minimises the compressive residual stresses resulting due to the transformation [19].

It has been found that the martensitic transformation does not

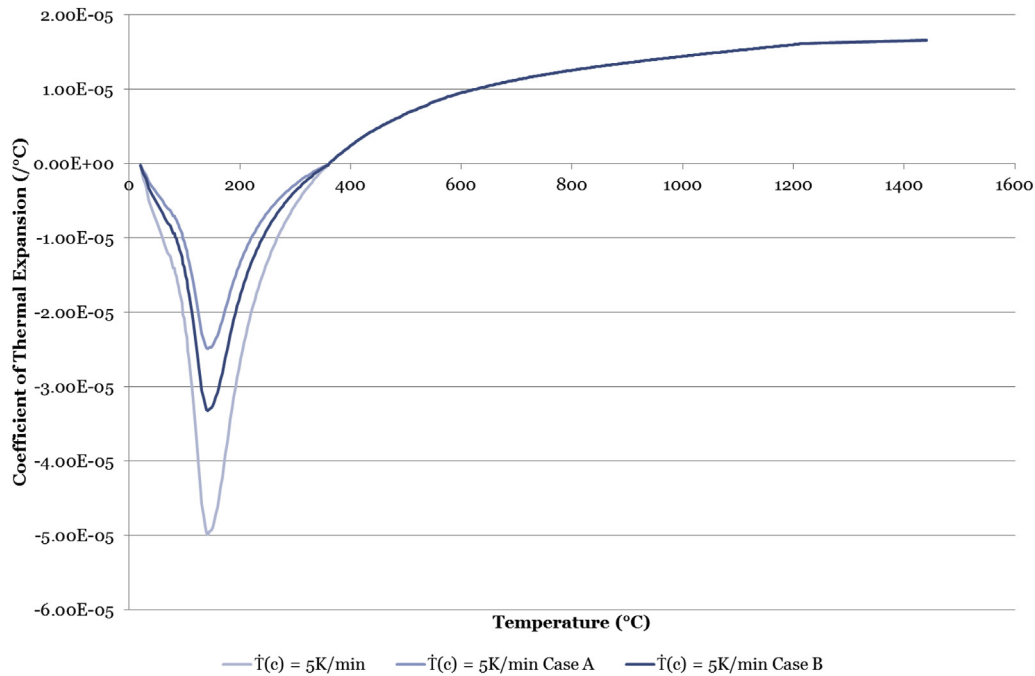


Fig. 9. Sensitivity study of coefficient of thermal expansion of 17–4 PH.

greatly affect residual stresses due to welding in low alloy carbon steels, however does greatly influence in the case of medium carbon steel [16]. This is relevant in the case of the use of 4330, explaining also why characterisation of 4330 is not as crucial as 17–4 PH. It is also likely that the substrate is of secondary importance due to decreased melting of the volume of material and the effect of alloying. Due to the importance of the martensitic transformation in the case of the clad material a sensitivity study of CTE values was undertaken and the residual stress distributions compared.

7.2. Influence of coefficient of thermal expansion on residual stresses

Fig. 10 presents the hoop stress along the horizontal path of the axisymmetric model for a 4330 clad with 17–4 PH using a pre-heat temperature of 150 °C. A study of variable sensitivity was achieved by dividing the data in the region of the martensitic phase change by 2 and 1.5 for cases A and B respectively. Focus is placed on the clad layer and the vicinity of the join. In this region it can be seen that in case A the hoop stress in the clad layer greatly decreases to result in a compressive residual stress around –200 MPa. In case B the hoop stresses are around –500 MPa in the clad layer therefore closer to the experimental residual stress measurement shown in Fig. 8. Fig. 11 more clearly illustrates the correlation between experimental and simulation hoop stresses when utilising the manipulated CTE data labelled as case B.

The study of the influence of CTE on residual stresses proves the requirement for temperature-dependent material properties that accurately capture the effects of cooling rate on the material properties and ultimately residual stresses. It may be that the manipulated data shown in Fig. 9 as case B represents the effects of the martensitic transformation on CTE due to the cooling rate during the weld cladding process. However it is clear that accurate testing would be the ideal scenario to erase the need for studies using manipulation of the data.

8. Discussion

In cyclically loaded components operating in a corrosive-erosive environment, the potential of the above fatigue-resistant coating and cladding concept is clear. While both the as-clad residual stresses and the autofrettage results for a plain cylinder have been successfully validated, it would be of interest to conduct experimental validation of the autofrettage simulation findings of Inconel 625 clad on a 4330 steel thick-walled cylinder. From both a simulation and experimental perspective, evaluation is required as to the advantages of using an Inconel 625 clad cylinder subjected to autofrettage, as opposed to a cylinder clad with 17–4 PH stainless steel. A 17–4 PH clad produces compressive residual stresses through the cladding process with no need for such a post-cladding operation. NACE regulations do not specifically consider the case of a clad layer with significant compressive residual stresses through the thickness. A highly compressive residual stress throughout the clad layer is likely to mitigate effects of cracking in a hydrogen sulphide environment and therefore this could be more desirable if materials utilised achieve required standards as dictated by NACE [4].

There are several key areas requiring further investigation in obtaining accurate residual stress distributions due to both the cladding and autofrettage processes.

8.1. Material hardening

An elastic-perfectly plastic material model has been used in this investigation and therefore in future both the weld cladding simulation and the autofrettage process should be developed to account for strain hardening.

Compressive residual stresses produced in the case of an elastic-perfectly plastic material model are thought to be higher than the stresses that would have been produced had a strain-hardening model been applied, as this was the case for an autofrettaged compound cylinder due to the Bauschinger effect [7].

The strain hardening potential of the materials under

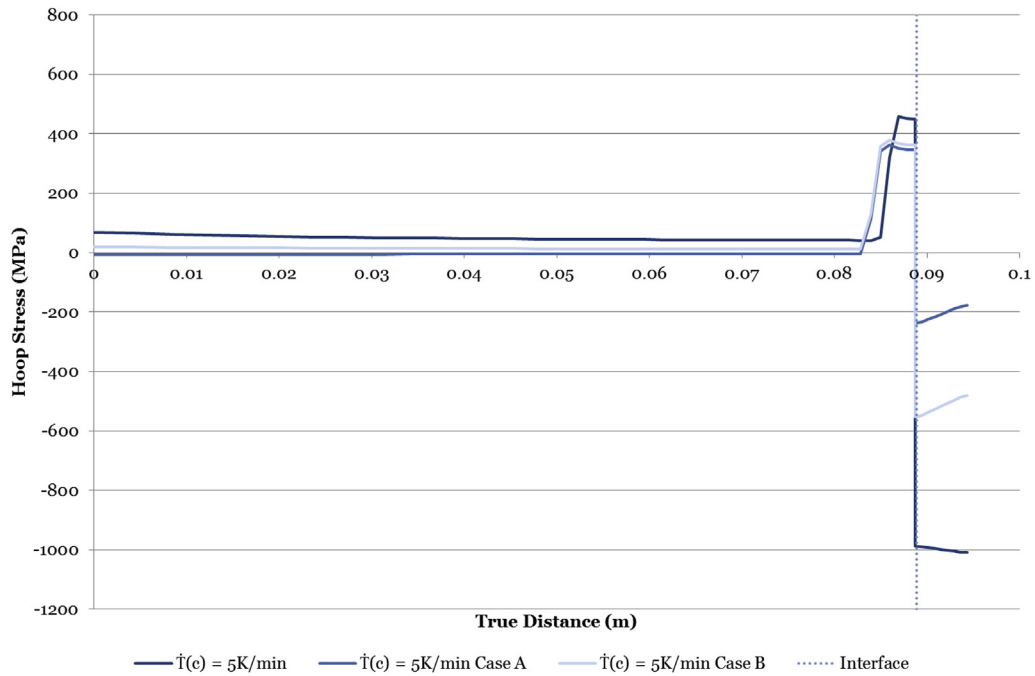


Fig. 10. Hoop residual stress distribution due to variation of CTE data – 17–4 PH clad cylinder.

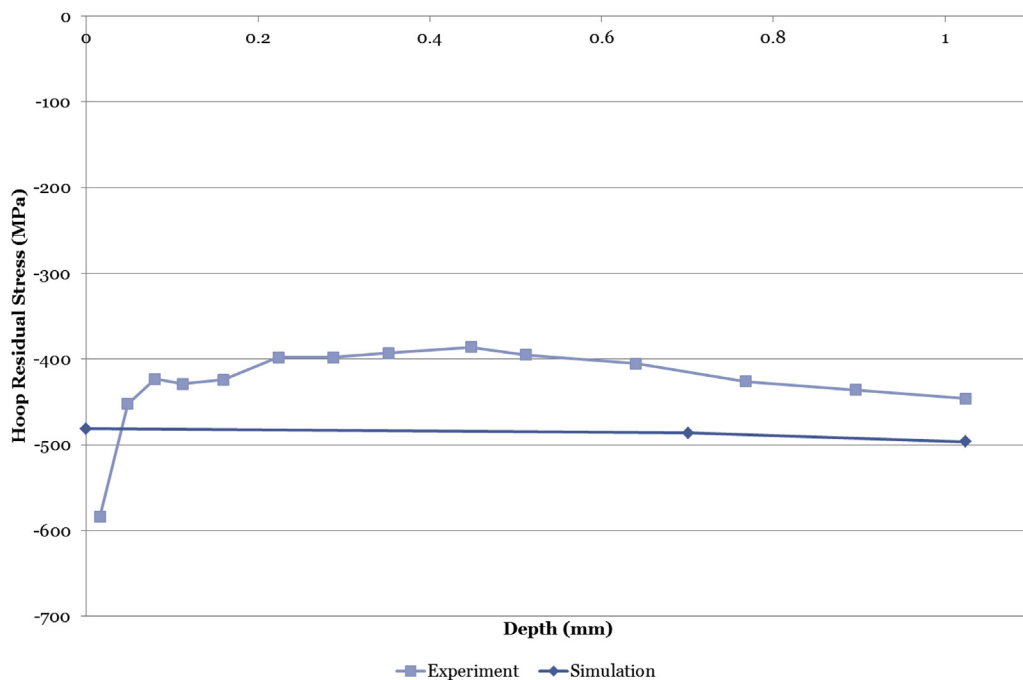


Fig. 11. Comparison of simulation and experimental hoop residual stress values due to variation of CTE data – 17–4 PH clad cylinder.

investigation was considered through calculation of the ratios of

Table 1

Tensile and yield strength ratios.

Material	UTS:YS
4330 (Inconel 625 clad)	1.170
4330 (17–4 PH clad)	1.180
Inconel 625	1.626

tensile strength to yield strength. The resulting values indicating the potential for the material to strain harden are provided in Table 1. These ratios were calculated using experimental data for representative as-clad and HAZ materials.

Table 2 provides the criteria presented by Pavlina and Van Tyne [20]. Strain hardening potential ranges indicate that both 4330 heat-affected zones (HAZ) and 17–4 PH have a low strain hardening potential, while Inconel 625 has a high strain hardening potential. The stress gradient in the plastic region is steeper for 17–4 PH than

Table 2
Strain hardening potential.

Ratio	Strain hardening potential
UTS:YS \leq 1.23	Low
1.23 < UTS:YS < 1.56	Medium
UTS:YS \geq 1.56	High

4330 as illustrated in the stress–strain trends provided in Refs. [21], demonstrating greater potential for 17–4 PH to strain harden. This suggestion further highlights the requirement to investigate material hardening both in reality and in the finite element model.

It should be noted that due to materials having little strength above a temperature of 800 °C, it is unlikely that the material properties will greatly impact the as-clad residual stress state at these temperature levels during the weld cladding process [22]. Therefore hardening will not be as prominent at higher temperatures. Model results using an elastic-perfectly plastic material model are shown in this paper to provide good correlation with experimental residual stresses, confirming the secondary importance of a hardening model at this stage. It is essential that material behaviour is not unintentionally influenced, for example by the use of inappropriate linear kinematic hardening models or inaccurate combinations of material properties [11].

A parametric study into multi-pass butt-welded stainless steel pipes highlighted that the hoop stress component appears more complex to capture due to increased sensitivity to constitutive models and the visible effects of phase transformations in this stress component [23]. This is the case in non-symmetrical modelling cases. In the case of modelling in an axisymmetric manner, stress components will not demonstrate such variations.

The weld material and material in the vicinity of the weld will experience reverse plastic yielding upon cooling. This requires consideration when implementing a hardening model as stresses will vary depending on the model used. The most commonly used model is the linear isotropic hardening model [13].

A study of Inconel 82/182 weld and buttering with 316L pipe and A508 forging concluded that hoop stresses were most accurately captured when using a mixed isotropic-kinematic hardening constitutive model. This is understandable as the inclusion of the Bauschinger effect and softening of the material will be the case in reality for a cyclically loaded component. Neglecting this will of course impact resulting stresses. Isotropic and kinematic hardening models resulted in conservative hoop stresses, although in the case of isotropic hardening stresses were most conservative [22]. This study in fact concluded that the constitutive model is one of the greatest influential factors in successfully modelling residual stress generation due to welding. However, this study investigates pressuriser nozzle dissimilar metal welds and therefore does not possess the same axisymmetric nature of the weld cladding process investigated herein.

A mixed isotropic-kinematic hardening model was further found to provide the most accurate post-weld residual stress field in a stainless steel slot weldment consisting of three passes [24].

Accounting for work hardening in a simulation model was however not found to produce great differences in resulting residual stresses in multi-pass butt-welded austenitic stainless steel pipes [25]. Therefore, it is difficult to conclude without further investigation and obtaining of accurate stress–strain data the influence of material hardening in the fatigue-resistant cladding technology.

Pre-cold working a material can be used to reduce the amount of strain hardening during machining. This may be possible using the autofrettage process, inducing compressive residual stresses whilst

easing machining, however further investigation is required here.

With regards to the application of autofrettage to a weld clad cylinder, the finite element model would also be developed to include a material model accounting for strain hardening, possibly Bauschinger effects as well as validity testing and experimental residual stress measurements. This validated finite element model would then be used to obtain production values for autofrettage pressures.

Good correlation for residual stresses has been presented between simulation and experiment in the case of an Inconel 625 clad, although the simulation model does not account for the strain hardening of the clad material. Although strain hardening potential has been indicated as low, due to the complexity of the modelling of the 17–4 precipitation hardening, martensitic clad material the effects of strain hardening should be investigated.

Ideally, experimental post-yield tensile test data would be used to derive a multi-linear hardening model. Access to limited published data [26] for a true stress–strain curve for non-welded substrate and clad materials would allow preliminary investigation into the effects of hardening on the cladding and autofrettage processes. However, it would also be desirable to experimentally obtain temperature-dependent strain hardening data. This could be undertaken using an electro-thermal mechanical test (ETMT) as described in Ref. [27]. Thermocouples and digital image correlation can be utilised to observe variations in strain during testing and specimens tested at required temperatures to obtain accurate representations of material hardening.

8.2. Assuming an idealised interface

Capturing accurate residual stress distributions through finite element modelling relies heavily upon detailed characterisation of the materials investigated. In the current model, an idealised interface is assumed such that two sets of material properties are assigned to the separate regions of the clad layer and the substrate. This does not account for diffusion and alloying effects due to the weld cladding process. It has been observed through metallurgical examination and experimental material property testing that both the microstructure and thermal and mechanical properties vary through the clad layer, HAZ and into the substrate. These variations are illustrated in the micro-section shown in Fig. 12.

Such assumptions will impact the residual stress distribution obtained. The residual stress distribution illustrated in Fig. 2 indicates large discontinuity stresses at the interface and these are likely to be exaggerated due to the fact that the effects of alloying and diffusion are not accounted for. Residual stress measurements

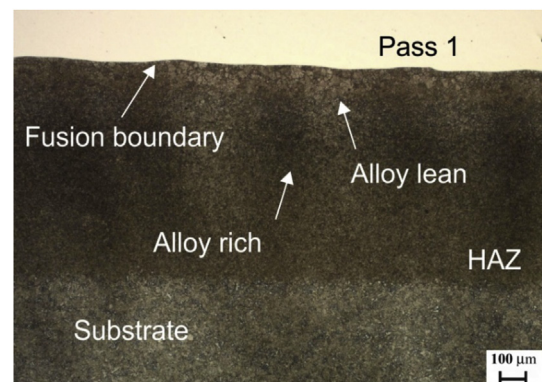


Fig. 12. Inconel 625 clad micro-section – illustrating varying microstructures due to alloying and diffusion.

obtained to a depth of 1 mm using ICHD do not provide results in this region and therefore alternative means of investigating residual stresses in the vicinity of the interface are required.

The contour method, a destructive method of residual stress measurement, was first introduced by Prime in 2001 [28]. The concept consists of the sectioning of the component causing the release of residual stresses. Measurement of the contour is undertaken followed by the forcing of the surface to the original state using a finite element model. This method is advantageous in that it allows measurement of macro stresses over a two-dimensional stress map of a component over the entire cut section [29]. The component can be of simple or complex geometry. Current investigation of the residual stresses in weld clad components is providing an insight into the residual stresses throughout the clad layer and across the clad-substrate interface. Fig. 13 illustrates the residual stress distribution obtained for a clad block. Tensile discontinuity stresses have been shown to be present in reality, however, to a lesser extent than indicated in the current finite element model. Nonetheless autofrettage will have beneficial effects on the as-clad residual stresses.

It is also expected that the results of the ICHD and contour method will provide a complimentary representation of the residual stress distribution in a weld clad component, as it has been shown that ICHD results provide results sensitive to surface stress fluctuation and the contour method will provide a detailed representation of stresses across the entire section.

8.3. Investigating residual stresses with depth

At present, as-clad residual stresses have been validated as well as autofrettage simulations for a plain cylinder benchmarked against available theoretical solutions. Validation is a key current area of investigation [11,30], and promise is also shown for studying the effects of autofrettage on a 17–4 PH clad on 4330 steel substrate. The stainless steel clad component does not strictly require autofrettage due to the compressive residual stress field present post-cladding, however it would of interest to investigate the effect of autofrettage on the discontinuity stresses at the clad-substrate boundary.

Prior to the investigation of autofrettage of a 17–4 PH clad component, further characterisation of the material would be required to ensure that simulation of the cladding and autofrettage process yields accurate residual stress distributions. It was shown in Fig. 9 that manipulation of the data was required to obtain good correlation with experimental results.

The contour method explained previously was used in obtaining residual stress measurements for the hoop stress component of the weld clad cylinder. Point indicators of the residual stresses obtained

are presented in Fig. 14. From this figure it can be seen that good correlation is obtained between the original simulation using experimentally obtained CTE data in the substrate. Alloying and diffusion has visibly lessened the discontinuity stresses at the interface and broadened the region in which interfacial effects are observed. In the clad layer hoop stresses obtained using the contour method match most closely with the results obtained through manipulation of the data in case A as illustrated in Fig. 9. This is contrary to correlation with the ICHD results therefore also indicating discrepancy between experimental results obtained using different methods.

Results presented using the contour method further prove that although characterization of 4330 low allow carbon steel is good and produces good correlation between experimental and simulation residual stresses, further characterization of 17–4 PH stainless steel is required prior to further studies into the effects of autofrettage of a component clad with this material. In fact a continuous process of validation and verification is the key to a robust understanding of the model as presented in Ref. [30].

8.4. Further considerations

In addition to the complexity of capturing material behaviour, the weld cladding process furthermore presents considerations in terms of the weld clad profile. At present experimental measurements of residual stress have been obtained on either a machined weld clad profile or the original weld clad profile. Machining of the weld clad profile will alter the residual stress present while operation of a weld clad component without machining will cause regions of stress concentration due to the peaks and troughs of the weld clad profile. Studies are currently being conducted as to the effects of the weld clad profile on residual stresses, in particular the ripple effect present on an as-clad component. Conducting autofrettage on such a surface would require the simulation to also account for the geometry of the weld clad profile. In turn this would result in increased complexity in the simulation however with the aim of improving the accuracy of the residual stress distribution obtained. Residual stresses arising due to the cladding process are greatly dependent on process parameters as discussed herein, for example material combinations and pre-heat and interpass temperatures. Factors such as clad layer depth, number of passes, cladding process and post-weld stress relief will also impact resulting residual stresses and present the opportunity to tailor the cladding process as discussed in Refs. [1], [5].

9. Conclusions

Mechanical autofrettage is shown to be a post-cladding process with the potential to significantly improve the residual stress distribution in a 4330 steel cylinder clad with Inconel 625. Results show the elimination of tensile residual stresses throughout the Inconel 625 weld clad. The potential also exists to eliminate the high discontinuity stresses at the clad-substrate boundary and induce compressive residual stresses well into the substrate. This will significantly enhance the fatigue performance of high strength 4330 components clad with Inconel 625.

In observing the effect of autofrettage pressure on hoop stresses, it is seen that an increase in pressure, between low and high pressure values, does not cause a notable difference in compressive residual stresses in the clad layer, limited due to the yield stress for the clad material. However the notable difference arises in the effect of autofrettage pressure on the discontinuity stresses at the interface and nature of residual hoop stress in the substrate. A lower autofrettage pressure results in a large discontinuity stress and even the higher autofrettage pressure applied is not large

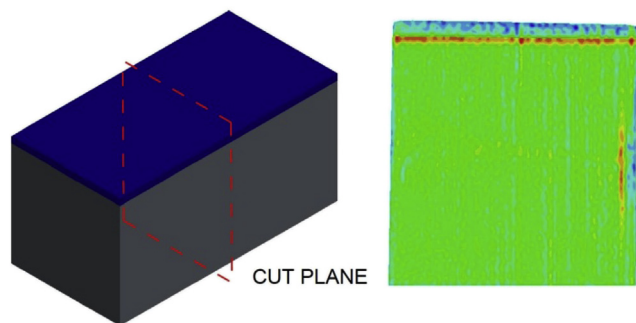


Fig. 13. Residual stress distribution obtained for a clad block – results courtesy of the Open University.

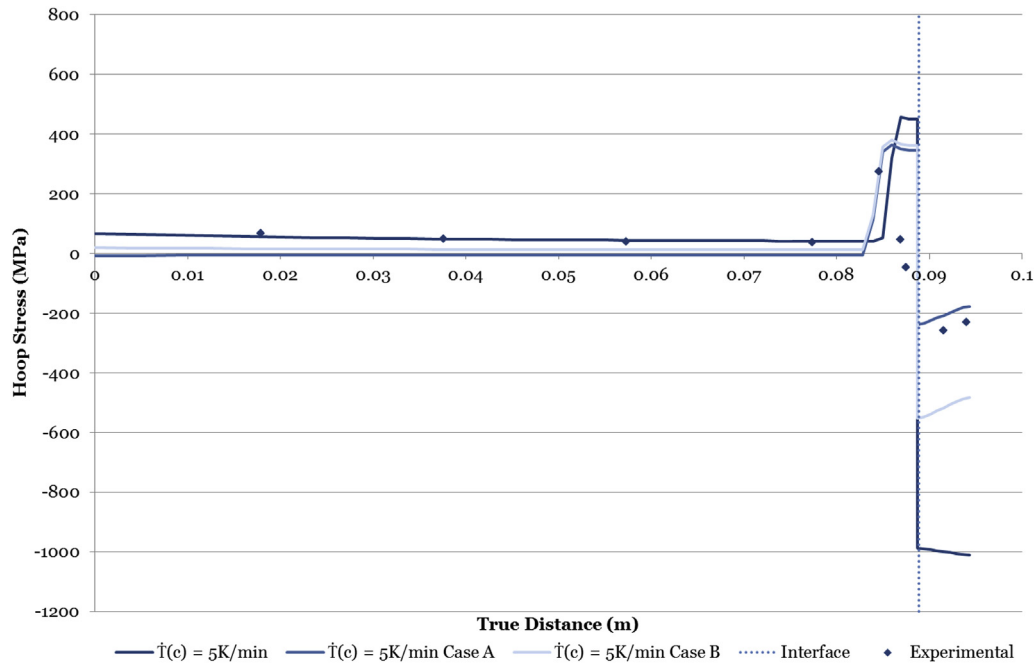


Fig. 14. Comparison of simulation and experimental hoop residual stress values using the contour method – 17–4 PH clad cylinder– experimental results courtesy of the Open University.

enough to yield the low alloy carbon steel substrate.

The findings presented do however successfully demonstrate the potential reduction of discontinuity stresses through the application of an autofrettage process.

For the purpose of a finite element model, pressure values can be adjusted as necessary and provide adequate information regarding the effects of autofrettage. However, in reality, for a real component with more complex geometry, it should be considered whether or not any proposed pressures are feasible, both economically and practically.

An alternative clad material has also been identified, producing compressive residual stresses in the clad layer. The use of 17–4 PH stainless steel is beneficial from a fatigue-resistance point of view however presents great difficulty in the simulation of the material behaviour due to the martensitic transformation upon cooling. This produces a discrepancy between experimental and simulation results. Sensitivity study results indicate that a reasonable variation in CTE data in the region of the martensitic transformation can produce good correlation with experimentally obtained residual stresses. This indicates that further characterisation of the material is required to capture the martensitic transformation in terms of effects on temperature-dependent material properties.

The effect of autofrettage on residual stresses and discontinuity stresses has been successfully demonstrated, however it is difficult to fully quantify without the implementation of a strain-hardening model. The effects of strain hardening have been discussed and strain hardening potential of the materials investigated evaluated using experimentally obtained data, indicating that Inconel 625 presents the greatest potential to strain harden. Good correlation has however been obtained between experimental and simulation residual stresses. Studies indicate varying degrees of importance in accounting for strain hardening depending on the nature of the welding process and component geometry. Therefore it is regarded as secondary in importance to implement a strain hardening model in the current axisymmetric finite element model.

Furthermore, the assumptions of an idealised interface are likely to result in larger discontinuity stresses than will be present in

reality. The contour method is currently being utilised to investigate the stress distribution throughout the clad component. Early indications presented show that the discontinuity stresses are indeed decreased in reality and furthermore that correlation between the original simulation using experimentally obtained data and contour method results is good in the substrate region. This proves yet again the need for further investigation into the behaviour and simulation of the martensitic stainless steel. Further considerations have been briefly discussed introducing aspects currently under investigation however the potential in the fatigue-resistant cladding concept is clear, whether utilising a combination of weld cladding and autofrettage or solely weld cladding with the correct material combination to yield compressive residual stresses in the clad layer.

Acknowledgements

The author would like to acknowledge the funding from the EPSRC (Grant no. EP/JF00550/1) and the Weir Group through the Weir Advanced Research Centre.

Associated Dataset

The data presented in this paper is available as a dataset at: <http://dx.doi.org/10.15129/b2bb7f32-7f37-41c4-aaa0-82a618419118>.

References

- [1] G. Schnier, J. Wood, A. Galloway, An experimental validation of residual stresses in weld clad pipelines, in: *Research and Applications in Structural Engineering, Mechanics & Computation: Proceedings of the Fifth International Conference on Structural Engineering, Mechanics & Computation*, 2013, pp. 613–617.
- [2] Wood J and Schnier G. Autofrettage of Thermally Clad Components. UK Patent Application GB 1501538.1, 2015.
- [3] ASTM International, Standard Test Method for Determining Residual Stresses by the Hole-drilling Strain-gage Method, 2008. West Conshohocken, Pennsylvania, E837–08e1.

- [4] NACE International, *Metals for Sulfide Stress Cracking and Stress Corrosion Cracking Resistance in Sour Oilfield Environments*, Houston, Texas, 2003.
- [5] G. Schnier, J. Wood, A. Galloway, Investigating the effects of process variables on the residual stresses of weld and laser cladding, *Adv. Mater. Res.* 996 (2014) 481–487.
- [6] F.A. Kandil, J.D. Lord, A.T. Fry, P.V. Grant, A review of residual stress measurement methods – a guide to technique selection, Teddington (2001). NPL Report MATC(A)04.
- [7] E.Y. Lee, Y.S. Lee, Q.M. Yang, J.H. Kim, K.U. Cha, S.K. Hong, Autofrettage process analysis of a compound cylinder based on the elastic-perfectly plastic and strain hardening stress–strain curve, *J. Mech. Sci. Technol.* 23 (2009) 3153–3160.
- [8] J.F. Harvey, *Theory and Design of Pressure Vessels*, Van Nostrand Reinhold Company Inc, New York, NY, 1985.
- [9] E.J. Hearn, *Mechanics of Materials 2, Third*, Butterworth-Heinemann, Oxford, 1997.
- [10] R. Ahmed, H. Yu, S. Stewart, L. Edwards, J.R. Santisteban, Residual strain measurements in thermal spray cermet coatings via neutron diffraction, *J. Tribol.* 129 (2) (2007) 411.
- [11] American Welding Society, *Guide for Verification and Validation in Computation Weld Mechanics*, 2013 vol. AWS A9.5:2.
- [12] Netzsch, *Netzsch Thermal Analysis, Netzsch DIL 402C*. [Online]. Available: <https://www.netzsch-thermal-analysis.com/en/>. [Accessed: 08-Dec-2015].
- [13] L.E. Lindgren, *Computational Welding Mechanics: Thermomechanical and Microstructural Simulations*, Woodhead Publishing Limited, Cambridge, UK, 2007.
- [14] A.H. Yaghi, T.H. Hyde, A.A. Becker, W. Sun, Numerical simulation of P91 pipe welding including the effects of solid-state phase transformation on residual stresses, *Proc. Inst. Mech. Eng. Part L J. Mater. Des. Appl.* 221 (4) (2007) 213–224.
- [15] D.J. Hornbach, P.S. Prevéy, P.W. Mason, X-ray diffraction characterization of the residual stress and hardness distributions in induction hardened gears, in: *First International Conference on Induction Hardened Gears and Critical Components*, 1995, pp. 69–76.
- [16] D. Deng, FEM prediction of welding residual stress and distortion in carbon steel considering phase transformation effects, *Mater. Des.* 30 (2) (2009) 359–366.
- [17] S.W. Ooi, J.E. Garnham, T.I. Ramjaun, Review: low transformation temperature weld filler for tensile residual stress reduction, *Mater. Des.* 56 (2014) 773–781.
- [18] M.T. Todinov, Influence of some parameters on the residual stresses from quenching, *Model Simul. Mater. Sci. Eng.* 7 (1999) 25–41.
- [19] M.C. Payares-Asprino, H. Katsumoto, S. Liu, Effect of martensite start and finish temperature on residual stress development in structural steel welds, *Weld. J.* 87 (2008) 279–290.
- [20] E.J. Pavlina, C.J. Tyne, Correlation of yield strength and tensile strength with hardness for steels, *J. Mater. Eng. Perform.* 17 (6) (2008) 888–893.
- [21] ASM International, *Atlas of Stress–Strain Curves, Second*, Materials Park, OH, USA, 2002.
- [22] M.C. Smith, O. Muransky, A. Goodfellow, E. Kingston, P. Freyer, S. Marlette, G.M. Wilkowski, B. Brust, S. Do-Jun, The impact of key simulation variables on predicted residual stresses in pressuriser nozzle dissimilar metal weld mock-ups. Part 2-comparison of simulation and measurement, in: *ASME PVP, 2010*, pp. 1–17.
- [23] B. Brickstad, B.L. Josefson, A parametric study of residual stresses in multi-pass butt-welded stainless steel pipes, *Int. J. Press Vessel. Pip.* 75 (1998) 11–25.
- [24] O. Muránsky, C.J. Hamelin, M.C. Smith, P.J. Bendeich, L. Edwards, The role of plasticity theory on the predicted residual stress field of weld structures, *Mater. Sci. Forum* 772 (2013) 65–71.
- [25] D. Deng, H. Murakawa, W. Liang, Numerical and experimental investigations on welding residual stress in multi-pass butt-welded austenitic stainless steel pipe, *Comput. Mater. Sci.* 42 (2008) 234–244.
- [26] MPDB, *JAHM Software Inc.*, 2013. www.jahm.com/.
- [27] B. Roebuck, M. Brooks, M.G. Gee, *Preliminary Elevated Temperature Mechanical Tests in the ETMT*, Teddington, UK, 1998.
- [28] M.B. Prime, Cross-sectional mapping of residual stresses by measuring the surface contour after a cut, *J. Eng. Mater. Technol.* 123 (2001) 162–168.
- [29] P.J. Withers, H.K.D.H. Bhadeshia, Residual stress: Part 1 – measurement techniques, *Mater. Sci. Technol.* 17 (2001) 355–365.
- [30] L.E. Schwer, *An Overview of the ASME Guide for Verification and Validation in Computational Solid Mechanics*, 2007.